JOURNAL OF VIROLOGY, Apr. 2005, p. 4709–4719 Vol. 79, No. 8
0022-538X/05/$08.00+0 doi:10.1128/JVI.79.8.4709–4719.2005

Association of Ebola Virus Matrix Protein VP40 with Microtubules

Gordon Ruthel,[1]† Gretchen L. Demmin,[1]† George Kallstrom,[1] Melodi P. Javid,[1] Shirin S. Badie,[1] Amy B. Will,[1] Timothy Nelle,[1] Rowena Schokman,[1] Tam L. Nguyen,[2] John H. Carra,[1] Sina Bavari,[1] and M. Javad Aman[1]*

United States Army Medical Research Institute of Infectious Diseases,[1] and Developmental Therapeutics Program, National Cancer Institute,[2] Frederick, Maryland

Received 1 October 2004/Accepted 16 December 2004

Viruses exploit a variety of cellular components to complete their life cycles, and it has become increasingly clear that use of host cell microtubules is a vital part of the infection process for many viruses. A variety of viral proteins have been identified that interact with microtubules, either directly or via a microtubule-associated motor protein. Here, we report that Ebola virus associates with microtubules via the matrix protein VP40. When transfected into mammalian cells, a fraction of VP40 colocalized with microtubule bundles and VP40 coimmunoprecipitated with tubulin. The degree of colocalization and microtubule bundling in cells was markedly intensified by truncation of the C terminus to a length of 317 amino acids. Further truncation to 308 or fewer amino acids abolished the association with microtubules. Both the full-length and the 317-amino-acid truncation mutant stabilized microtubules against depolymerization with nocodazole. Direct physical interaction between purified VP40 and tubulin proteins was demonstrated in vitro. A region of moderate homology to the tubulin binding motif of the microtubule-associated protein MAP2 was identified in VP40. Deleting this region resulted in loss of microtubule stabilization against drug-induced depolymerization. The presence of VP40-associated microtubules in cells continuously treated with nocodazole suggested that VP40 promotes tubulin polymerization. Using an in vitro polymerization assay, we demonstrated that VP40 directly enhances tubulin polymerization without any cellular mediators. These results suggest that microtubules may play an important role in the Ebola virus life cycle and potentially provide a novel target for therapeutic intervention against this highly pathogenic virus.

The reliance of viruses on host cell machinery typically extends beyond actual replication of the viral genome to include trafficking of the virus to the site of replication and egress of viral progeny out of the cell. Directed transport within the cell occurs along cytoskeletal tracks, primarily microtubules, although some transport is also supported by actin microfilaments. Microtubules can be important not only for early or late events such as transport to the nucleus or transit to sites of budding at the plasma membrane but also for shuttling intermediate viral products between sites of assembly within the cell (10, 49). In addition to transport functions, microtubules have been of interest as a potential scaffold for viral assembly (44). In fact, tubulin has been shown to be an important regulator of transcription for several negative-strand RNA viruses (6, 9, 20, 35, 42, 54, 58).

Evidence for an association between viruses and host cell cytoskeletal elements was reported as early as the 1970s (30, 31). In recent years, there has been a resurgence of interest in virus-cytoskeleton interactions that has culminated in several reviews on the topic (36, 46, 52). In addition to a mounting number of viruses reported to make use of the host cell cytoskeleton, specific viral proteins that interact either directly with microtubules or with microtubule-associated motor proteins have begun to be identified. These include the tegument protein VP22 of herpes simplex virus type 1 (13, 32), VP22 of Marek's disease virus (41), M protein of Sendai virus (42), L protein of Theiler's murine encephalomyelitis virus (40), A36R membrane protein of vaccinia virus (57), protein p54 of African swine fever virus (1), spike protein VP4 of rotavirus (39), and core protein μ2 of reovirus (44).

The filovirus Ebola (EBOV) is a nonsegmented, negative-strand RNA virus that causes severe, often fatal, hemorrhagic fever in humans and other primate species. The periodic occurrence of natural outbreaks and the potential for weaponization, combined with a lack of preventative or therapeutic measures, make EBOV a serious public health concern. Although progress has been made toward understanding the EBOV infection process and how the virus traffics through the cell (2, 14), much remains unknown. In particular, the molecular mechanisms of filovirus assembly and its possible interactions with cellular components such as the cytoskeletal network are poorly understood.

The matrix proteins of the negative-strand RNA viruses are involved in viral egress, playing a critical role in assembly and budding (17). The Ebola virus matrix protein VP40 consists of two structurally similar domains with a β-sandwich structure (11). Purified VP40 protein has been shown to form oligomers when bound to lipid bilayers or destabilized by C-terminal truncations (48, 50). When transfected into cultured cells in the absence of other viral proteins, VP40 becomes localized to the plasma membrane lipid rafts (43), suggesting a possible further role for VP40 in the trafficking of replicated virus to the membrane. Ectopic expression of VP40 results in the formation of filamentous, virus-like particles, suggesting that VP40 is the main driving force for final particle assembly (4, 21, 55). Our previous studies indicated that a fraction of Ebola VP40

* Corresponding author. Mailing address: USAMRIID, 1425 Porter St., Frederick, MD 21702. Phone: (301) 619-6727. Fax: (301) 619-2348. E-mail: amanm@ncifcrf.gov.

† These authors contributed equally to this work.

remains in the cytoplasm, possibly associated with cellular compartments (43). Several motifs in the VP40 molecule can potentially mediate interaction with cellular proteins (2), but except for the domains interacting with the vacuolar protein sorting machinery (19, 33), the functional significance of these motifs has not been examined. In this report, we present evidence that Ebola VP40 associates with microtubules and that transfection of cells with VP40, or infection with EBOV, rearranges and stabilizes microtubules. We also identify a motif within the VP40 sequence that may represent a basis for the interaction of VP40 with tubulin.

MATERIALS AND METHODS

VP40 mutation and transfection. Tagging of VP40 and production of VP40 truncation mutants were described previously (43). Briefly, a tetracysteine (TC) tag (16) was added to the N terminus of VP40 cDNA (TC-VP40$_{1–326}$) to allow visualization with the biarsenic fluorophore FlAsH. TC-VP40$_{1–326}$ was used as a template to generate truncation mutants with a Stratagene QuickChange kit. The constructs were transfected into 293T, Vero-E6, GHOST, and HEP-G2 cells by using Lipofectamine plus (Invitrogen, Carlsbad, Calif.) according to the manufacturer's instructions.

Fluorescent labeling and confocal microscopy. Tetracysteine-tagged Ebola VP40 and mutants thereof were labeled by using FlAsH (Panvera, Madison, Wis.) as previously described (16, 43). In some instances, the Lumio Green kit (Invitrogen) was used for FlAsH labeling per the manufacturer's instructions. In other cases, VP40 was visualized by a rabbit antibody to the C-terminal 16 amino acids of Ebola VP40 (43). However, we found antibody staining to be less effective than FlAsH staining for labeling microtubule-associated VP40, perhaps due to masking of antibody epitopes by microtubule association. The same antibody was also used to visualize VP40 in Ebola-infected cells. Cells were moved into a containment suite, infected, fixed in 4% formaldehyde, and irradiated to kill the virus before being stained for confocal microscopy. Microtubules were labeled with DM1A anti-α-tubulin monoclonal antibody (1:500; Sigma, St. Louis, Mo.) and an Alexa 568-conjugated goat anti-mouse secondary antibody (1:500; Molecular Probes, Eugene, Oreg.). Cell nuclei were labeled with Hoechst stain (Molecular Probes). Images were obtained with a Bio-Rad (Hercules, Calif.) 2000MP confocal/multiphoton system attached to a Nikon TE300 inverted microscope.

Immunoprecipitation and Western blots. 293T cells, transfected with VP40, were lysed in lysis buffer containing 1% Triton X-100, 150 mM NaCl, 10 mM Tris-HCl (pH 7.5), 1 mM $MgCl_2$, and 1 mM EGTA at room temperature. Tubulin was immunoprecipitated from cell lysates with DM1A anti-α-tubulin monoclonal antibody and magnetic beads coated with goat anti-mouse antibody (Dynal, Brown Deer, Wis.). Cell lysates and immunoprecipitates were analyzed by sodium dodecyl sulfate-polyacrylamide gel electrophoresis and immunoblotting with rabbit anti-VP40 (43) or sheep anti-tubulin antibodies (Cytoskeleton, Denver, Colo.).

Generation of purified VP40 and tubulin binding assay. Ebola VP40$_{1–326}$ was cloned into pET22b vector (Novagen, San Diego, Calif.) and expressed in *Escherichia coli* strain BL21(DE3) for purification (11). Cells were induced in log phase at 37°C with 0.1 mM isopropyl-β-D-thiogalactopyranoside (IPTG) and grown for an additional 4 h at 30°C. Harvested cells were lysed by microfluidization in 50 mM Tris (pH 8.8), 100 mM NaCl, and 0.1 mM β-mercaptoethanol (lysis buffer) containing Complete EDTA-free protease inhibitor (Roche Diagnostics, Indianapolis, Ind.). Cell debris in the lysate was removed by centrifugation, and 0.17% polyethyleneimine was added to the supernatant. The sample was centrifuged again, and the supernatant was applied to a Q-Sepharose column (Amersham Biosciences, Piscataway, N.J.). Ebola VP40 in the flowthrough was pelleted by precipitation with 50% $(NH_4)_2SO_4$ solution in a 2:1 (vol/vol) ratio. The pellet was resuspended in lysis buffer and dialyzed overnight into buffer containing 20 mM bicine (pH 9.3), 100 mM NaCl, and 0.1 mM β-mercaptoethanol before final purification by sizing chromatography (Sephacryl S-200; Amersham Biosciences) (11). To generate oligomeric VP40, purified His-tagged VP40 was incubated with 2 M urea and an excess of *E. coli* nucleic acids as described previously (18) and isolated by sizing chromatography (Sephacryl S-200; Amersham Biosciences).

Two different approaches were used for the tubulin binding assay. First, a mixture of purified VP40 and tubulin in phosphate-buffered saline (PBS) was subjected to immunoprecipitation followed by immunoblotting, as described above, to detect direct physical association between the two proteins. In a second approach, purified VP40 (20 μg/well) was immobilized on MaxiSorb 96-well plates (Nunc, Roskilde, Denmark) or Ni^{2+}-coated plates (Pierce, Rockford, Ill.). After blocking the nonspecific binding sites with 5% nonfat milk, various amounts of purified tubulin (Cytoskeleton) were added to the wells and incubated at room temperature for 2 to 3 h. After washing the unbound protein, bound tubulin was detected by DM1A monoclonal antibody followed by horseradish peroxidase (HRP)-conjugated anti-mouse antibody and horseradish peroxidase detection reagents. Binding was measured in an enzyme-linked immunosorbent assay reader as absorbance at 405 nm.

In vitro polymerization of tubulin. Tubulin polymerization assays were performed with a kit purchased from Cytoskeleton, Inc., by using the protocol recommended by the manufacturer. The polymerization was monitored in real time in the presence and absence of VP40 or a control protein by measuring the light scattering at 340 nm over several hours.

Ebola virus infection. Vero-E6 or 293T cells were infected at a multiplicity of infection of 1 with Ebola Zaire virus for 50 min at 37°C, 5% CO_2 in eight-well chamber slides. Nonadsorbed virus was removed from cells by washing monolayers twice with PBS followed by addition of fresh complete medium for an additional 48 h. Samples were fixed in 4% formaldehyde, inactivated by irradiation (10^7 R, ^{60}Co source), and tested for absence of infectivity in cell culture before use.

RESULTS

VP40 associates with cellular microtubules and purified tubulin. In a previous study (43), we noted that a fraction of Ebola VP40 transfected into 293T cells was often arranged in a fibrillar pattern inside the cells. Although this pattern was often present in full-length VP40, it became extremely consistent and dramatic after truncating the C-terminal nine amino acids (VP40$_{1–317}$). The resemblance to microtubule bundles and the similarity in pattern to microtubule-associated viral proteins such as VP22 of herpes simplex virus type 1 (13, 32) and μ2 of reovirus (5, 44) led us to investigate whether this pattern of VP40 cellular localization reflects association with microtubules. We therefore compared the immunofluorescence localization pattern of α-tubulin to the distribution pattern of VP40, visualized with an N-terminal tetracysteine tag and the biarsenic dye FlAsH as previously described (16, 43). As shown in Fig. 1, these experiments revealed considerable colocalization of full-length VP40, as well as VP40$_{1–317}$, with microtubules. Examination of the tubulin staining pattern further revealed a readily noticeable bundling of microtubules in cells expressing the full-length VP40 compared to untransfected cells (compare Fig. 1 with the first panel of Fig. 5A). The microtubule bundling was even more pronounced in cells transfected with the VP40$_{1–317}$ truncation mutant. Further truncation of VP40 at residue 308 (VP40$_{1–308}$),a mutation that completely eliminates the release of VP40-containing Ebola virus-like particles (43), eliminated the colocalization with microtubules as well as the aberrant formation of microtubule bundles (Fig. 1). VP40$_{1–308}$ was arranged in a globular pattern typically located close to the nucleus, as we had reported previously (43). Similar results to those described above were obtained when VP40, VP40$_{1–317}$, and VP40$_{1–308}$ were transfected into Vero-E6, GHOST, or HEP-G2 cells (data not shown). It must be noted that the microtubule-associated VP40 was less readily detectable by our antibody staining than by FlAsH staining (see Fig. 8), possibly due to poor accessibility of the epitope in the complex. However, most cells staining positive for VP40 consistently displayed bundling of microtubules independent of staining technique (see Fig. 8 and data not shown).

Because some viruses known to associate with microtubules

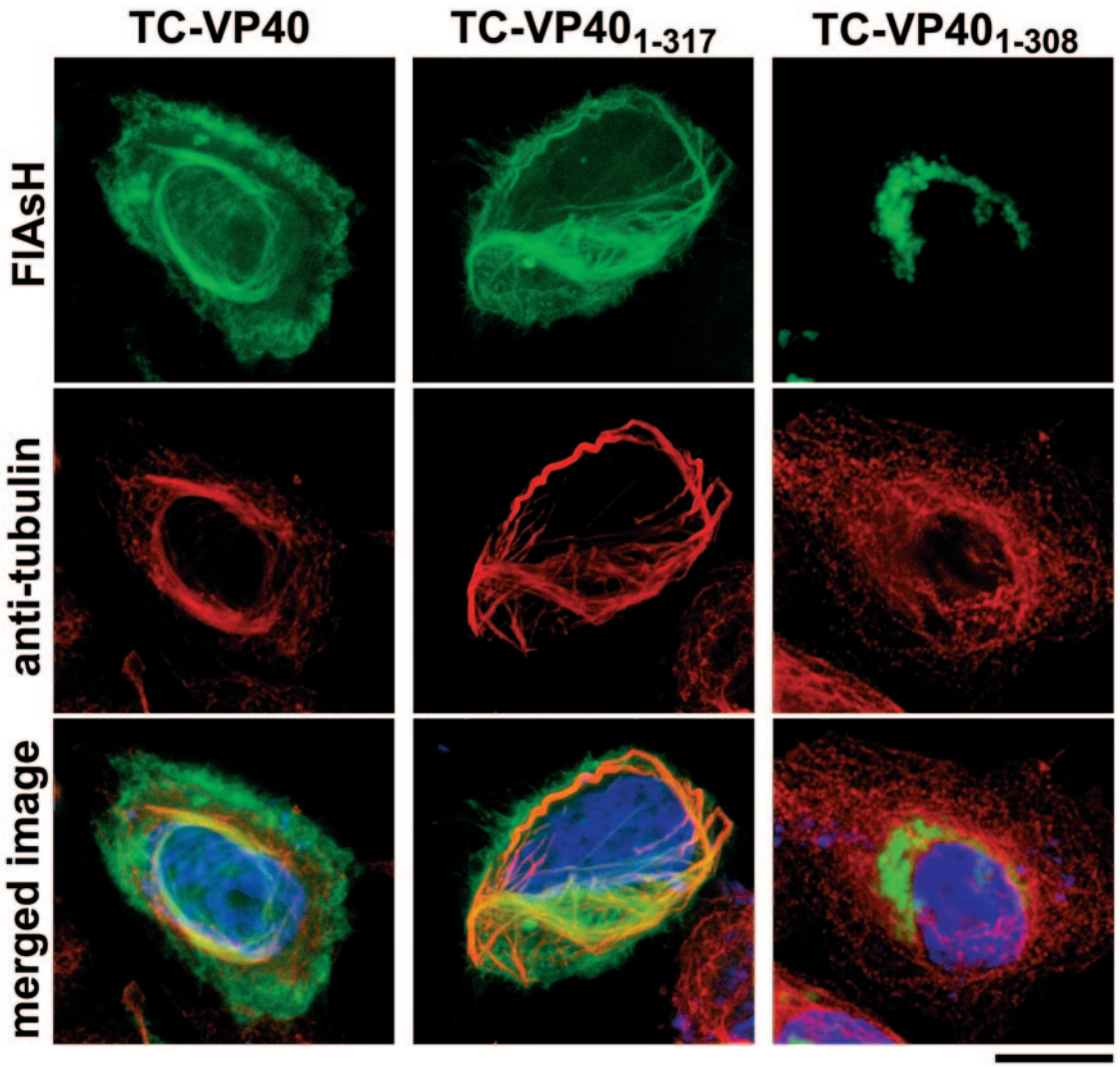

FIG. 1. Colocalization of VP40 with microtubules. Tetracysteine-tagged, full-length VP40 (left), VP40$_{1–317}$ (middle), and VP40$_{1–308}$ (right) were transfected into 293T cells and visualized with FlAsH (green). The cells were then fixed and labeled with an antibody to α-tubulin (red) and stained with Hoechst stain (blue) to show the nucleus. Microtubule bundles can be seen associated with full-length VP40 and VP40$_{1–317}$ but not VP40$_{1–308}$. Bar, 10 μm.

have also been reported to localize to the microtubule organizing center or centrosome (3, 45), we examined VP40 localized at or near regions enriched in γ-tubulin, a prominent constituent of centrosomes. However, examination of a large number of cells revealed no colocalization between VP40 and γ-tubulin (Fig. 2A), nor was microtubule-associated VP40 reliably clustered around γ-tubulin.

VP40 is known to interact with the vacuolar protein sorting (*vps*) protein TSG101, causing its redistribution to the plasma membrane and lipid rafts (33, 43). This interaction is proposed to be critical for the vesicular budding of VP40 (28). However, it is not known whether TSG101 plays any role in VP40 trafficking. Recently, Chiou and colleagues reported the concurrent association of TSG101 and the NS3 protein of the Japanese encephalitis virus with microtubules (7). Therefore, we examined the pattern of TSG101 immunofluorescence to determine whether TSG101 colocalized with microtubule-associated VP40. While TSG101 was clearly redirected to the plasma membrane in the presence of VP40, it did not exhibit any association with the bundled microtubules (Fig. 2B). These data suggest that while bound to microtubules, the late (L) domain of VP40 may be sterically hindered for interaction with TSG101. The finding further suggests that TSG101 probably does not play a major role in VP40 subcellular trafficking to the plasma membrane.

To further examine the physical association between microtubules and VP40, we performed immunoprecipitation studies. Cells were transfected with a control plasmid or cDNA for full-length VP40, and tubulin was immunoprecipitated from cell lysates made in a microtubule-stabilizing buffer. As shown in Fig. 3A, VP40 coimmunoprecipitated with anti-α tubulin monoclonal antibody (MAb), suggesting a physical association of VP40 with tubulin. Modest levels of association in cell lysates may reflect the fact that the majority of the polymerized tubulin was lost to the pellet after lysis and centrifugation. These data, along with the colocalization studies, clearly dem-

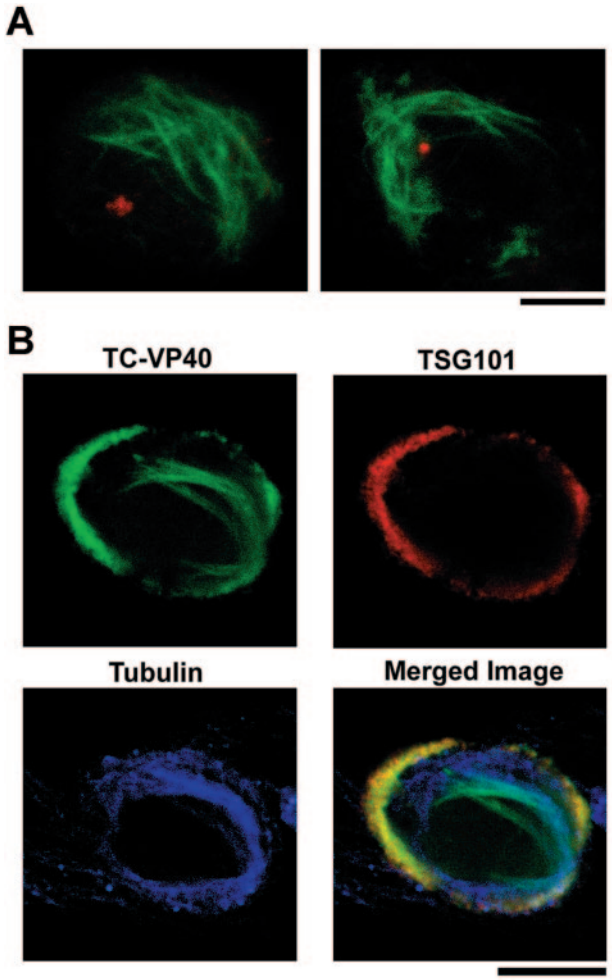

FIG. 2. VP40 arranged along microtubules does not associate with centrosomes or TSG101. (A) TC-VP40$_{1–317}$ was transfected into 293T cells and stained with FlAsH (green). Cells were subsequently fixed and immunostained with an antibody to γ-tubulin to mark the location of centrosomes. (B) 293T cells expressing full-length TC-VP40 were stained with FlAsH (green) and immunostained with antibodies to TSG101 (red) and α-tubulin (blue). As seen in the merged image, fractions of VP40 colocalized with TSG101 or with microtubules, but little or no colocalization occurred among all three. Bars, 10 μm.

onstrate a physical interaction between VP40 and microtubules. To address whether this interaction occurs directly between VP40 and tubulin or is mediated by a microtubule-associated protein, we immunoprecipitated tubulin from a mixture of purified tubulin heterodimers and purified full-length VP40. As shown in Fig. 3B, anti-tubulin MAb pulled down VP40 in addition to the purified tubulin, indicating a direct interaction between the two proteins. To further confirm the direct association of the two proteins, we immobilized purified VP40 on 96-well plates and incubated the plates with different amounts of purified tubulin. After an extensive wash, bound tubulin was detected by anti-tubulin and HRP-conjugated secondary antibodies. As shown in Fig. 3C, a specific, dose-dependent binding between VP40 and tubulin was detected in this experiment. Taken together, these studies indicate that the association of VP40 with microtubules is a consequence of direct interaction with tubulin. In addition, the data suggest that VP40 can interact with both the polymerized and heterodimeric tubulin.

We then sought to determine whether tubulin has a preference with respect to monomeric or oligomeric VP40. For this purpose, we generated oligomeric VP40 by addition of RNA to monomeric His-tagged VP40 as described previously by Gomis-Ruth and colleagues (18). Figure 4A shows the monomeric and in vitro-oligomerized VP40 proteins. The proteins were then immobilized on Ni^{2+}-coated plates and incubated with different amounts of tubulin, and bound tubulin was detected by anti-tubulin antibody. As shown in Fig. 4B, in this experiment we did not detect any significant difference in binding of the monomeric and oligomeric VP40 to tubulin.

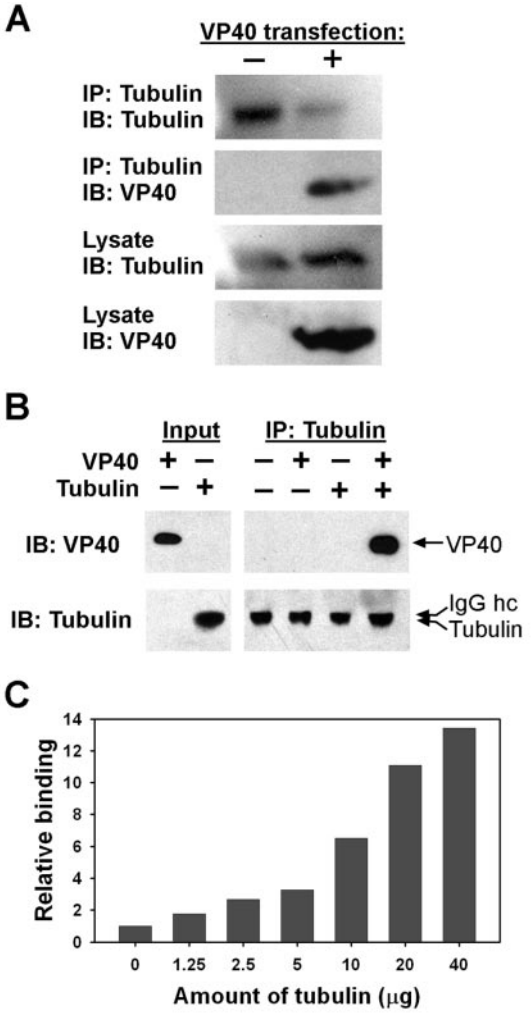

FIG. 3. Physical association between VP40 and tubulin. (A) 293T cells were transfected with VP40 (+) or a control DNA (−) and lysed after 48 h in a microtubule-stabilizing buffer. Tubulin was immunoprecipitated (IP) by DM1A MAb, and lysates and immunoprecipitates were analyzed by immunoblotting (IB) with the indicated antibodies. (B) Purified tubulin and VP40 were mixed in PBS and subjected to immunoprecipitation and immunoblotting. IgG, immunoglobulin G. (C) VP40 was immobilized on 96-well plates (10 μg/well), different amounts of tubulin were added, and after binding and washing, bound tubulin was assayed by DM1A and HRP-conjugated anti-mouse antibody. Data represent the enzyme-linked immunosorbent assay reading converted to relative binding.

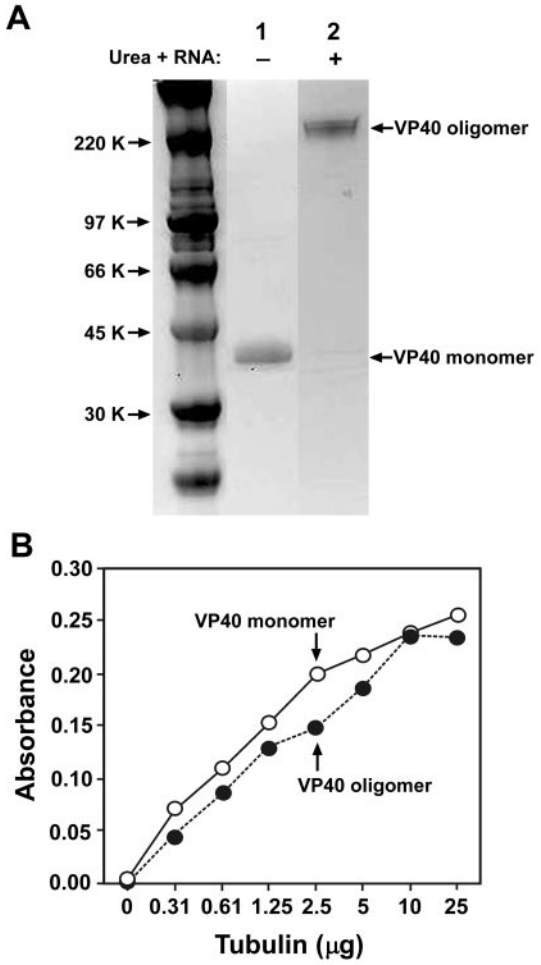

FIG. 4. Binding of tubulin to monomeric and oligomeric VP40. (A) SDS-PAGE analysis of monomeric and oligomeric His-tagged Ebola $VP40_{31–326}$. Monomeric His-tagged Ebola $VP40_{31–326}$ (lane 1) was incubated with 2 M urea and an excess of *E. coli* nucleic acids to form oligomers (lane 2) and isolated by sizing chromatography. (B) Two micrograms of His-tagged monomeric or oligomeric VP40 was bound to Ni^{2+} plates and, after blocking, incubated with the indicated amounts of purified tubulin. Plates were washed, and bound tubulin was detected with an anti-tubulin MAb, HRP-conjugated anti-mouse antibody, and chromogenic reagents.

VP40 association stabilizes cellular microtubules against drug-induced depolymerization. Having determined an association between VP40 and microtubules, we expected that depolymerization of microtubules may redistribute VP40. However, treating cells with moderate concentrations of the microtubule-depolymerizing drugs nocodazole or colchicine yielded a very different result. We found that microtubule bundles that colocalized with VP40 were largely protected against drug-induced depolymerization when incubated for 2 h with nocodazole (Fig. 5A and B). Identical results were obtained when the cells were treated continuously with nocodazole starting 1 h after transfection (Fig. 5C), suggesting that VP40 may actively promote the polymerization of tubulin in the presence of depolymerizing drugs, as well as protecting the existing polymer from disruption.

Polymerization of tubulin is enhanced by purified VP40. To test the ability of VP40 to promote tubulin polymerization, we performed an in vitro tubulin polymerization assay with purified proteins. This assay takes advantage of the increase in light scattering at 340 nm as a result of tubulin polymerization. As shown in Fig. 6, adding purified VP40 to a tubulin polymerization reaction significantly increased the rate of microtubule polymerization in a dose-dependent manner. VP40, at a ratio of 1:12 (VP40 to tubulin), increased the maximum light scattering in this reaction and decreased the time to reach the maximal polymerization by 50% (Fig. 6). This effect did not result from a change in light scattering caused by VP40 itself during the incubation time, as a control containing VP40 without tubulin showed no increase in light scattering (Fig. 6). The effect was specific to VP40, as adding 25 μg of bovine serum albumin did not affect the rate of microtubule formation (Fig. 6). To the best of our knowledge, this is the first report of an animal virus protein directly promoting tubulin polymerization in vitro.

VP40 contains a motif homologous to MAP2 tubulin binding motif. Having determined that VP40 interacts directly with tubulin, we sought a molecular basis for this interaction. The bundling and stabilization of microtubules by VP40 strikingly resemble the effect exerted by some microtubule-associated proteins such as MAP2 and Tau (15, 23). Four 31-amino-acid imperfect repeats in MAP2 are known to be critical for the association with microtubules (15, 29). When we performed alignments of VP40 with the MAP2 repeats, we found a region in VP40 (amino acids 223 to 253) with 35% sequence identity and 39% homology with the MAP2 fourth repeat (Fig. 7A). As shown by the X-ray structure of VP40 (Fig. 7B), residues 223 to 253 lie on the surface of the protein structure and, accordingly, could provide a binding surface for tubulin. To examine a possible involvement of this region in association with microtubules and microtubule bundling, we used two deletion mutants of VP40 lacking amino acids 226 to 240 or 241 to 255. These mutants and a wild-type control were transfected into 293T cells, and 48 h hours after transfection, cells were treated with 10 μM nocodazole for 2 h before staining for tubulin and VP40. As shown in Fig. 7C, while the wild-type VP40 protected microtubules from depolymerization, these two mutants did not. It is noteworthy that these mutants also failed to associate with the plasma membrane. These data suggest that VP40 may use amino acids within the regions deleted in these mutants, which essentially cover the potential tubulin binding sequences (223 to 254) to influence microtubule dynamics in a manner similar to MAP2.

Ebola virus infection results in rearrangement of microtubules into bundles. While the transfection experiments suggested an involvement of microtubules in EBOV cellular trafficking, it was important to demonstrate this phenomenon in the context of infection with the authentic virus. Therefore, we examined the microtubules of EBOV-infected 293T and Vero-E6 cells. Cells were infected with Ebola Zaire and, 48 h after infection, were treated with nocodazole, fixed, irradiated, and stained. As shown in Fig. 8, infected cells contained numerous, thick bundles of microtubules, suggesting that VP40 produced during an EBOV infection has a similar effect on microtubules to what we observed in VP40-transfected cells. Although Vero-E6 cells are shown in Fig. 8, similar results were obtained with 293T cells. In general, we noted that microtubule bundling in the infection experiments was less dra-

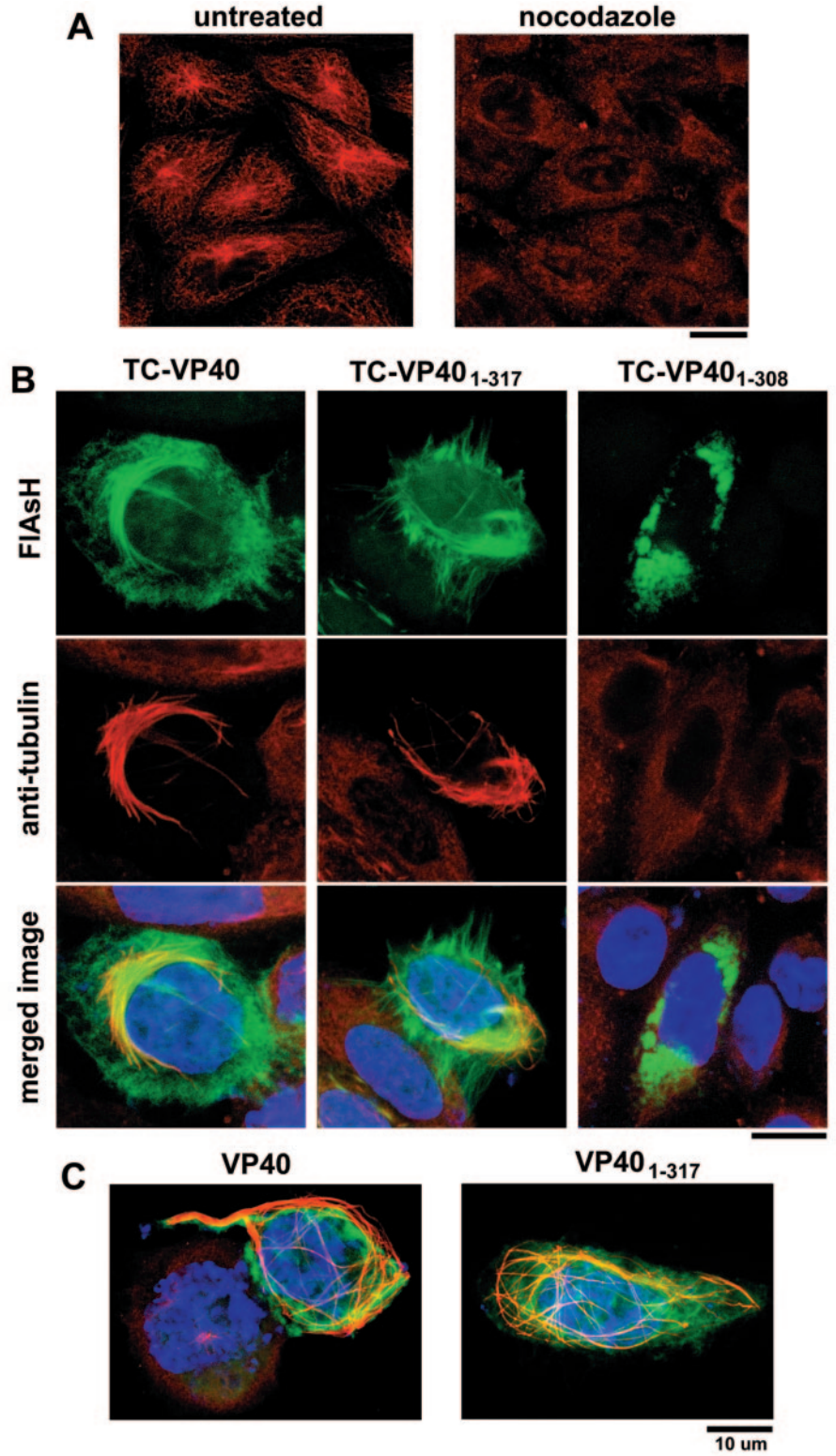

FIG. 5. VP40 stabilizes microtubules against nocodazole-induced depolymerization. (A) 293T cells immunostained for α-tubulin demonstrate the effect of a 2-h incubation in nocodazole (right) compared to untreated cells (left). (B) Nocodazole (2 μM) was applied to 293T cells transfected with TC-VP40$_{1–317}$ (middle) or TC-VP40$_{1–308}$ (right) for 2 h before fixation. VP40 was visualized with FlAsH (green), and after fixation, the cells were immunolabeled for α-tubulin (red) and stained with Hoechst dye to show cell nuclei. Microtubules are retained in cells expressing full-length VP40 or VP40$_{1–317}$ but not VP40$_{1–308}$. (C) Microtubules can be seen in abundance in cells expressing VP40 or VP40$_{1–317}$ even when cells are treated continuously with nocodazole from within 1 h after transfection. The panel for full-length TC-VP40 also contains a nonexpressing cell for comparison. Bars, 10 μm.

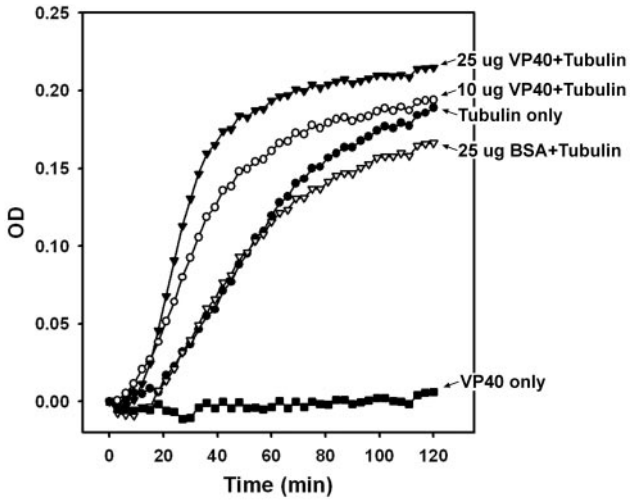

FIG. 6. VP40 promotes tubulin polymerization. The tubulin polymerization assay (see Materials and Methods) was performed in the presence of VP40 or bovine serum albumin (BSA), and polymerization was monitored by light scattering at 340 nm. All data points represent the light scattering of each sample corrected for background (starting point) levels of the same sample. The VP40-only control contains VP40 but no tubulin. Data were recorded for 2 h at 37°C at 3-min intervals. OD, optical density.

matic than what we observed with VP40 transfection. This may reflect modulation of VP40-microtubule interaction by the remaining Ebola proteins or may result from the handling of samples before removal from BSL4. For safety reasons, infected cells undergo very harsh treatments such as fixation in acetone, incubation at −80°C for several days, and irradiation (6×10^6 rad) before leaving the biocontainment laboratory. Therefore, the reduced level of bundling in these cells, compared to transfection experiments, may be a result of microtubule destabilization during these treatments. Nevertheless, the data strongly support the association of microtubules with Ebola proteins during the viral life cycle.

DISCUSSION

The results described above demonstrate that Ebola VP40 associates with microtubules through a direct interaction with tubulin. This association reorganizes microtubules into bundles and stabilizes them against drug-induced depolymerization, similar to what has been reported for the herpes simplex virus protein VP22 (13, 32), reovirus μ2 (5, 44), and NS3 of the Japanese encephalitis virus (7). Our results further indicate that infection with the live EBOV likewise bundles and stabilizes microtubules, although to a lesser degree than what is seen with VP40 transfection. This study is also the first report of an animal viral protein that can directly enhance tubulin polymerization in vitro. Taken together, our findings suggest that EBOV employs microtubules during its life cycle, a phenomenon that appears to be conserved across a number of viral families (46).

While colocalization with cellular microtubules has been reported for several viral proteins, to the best of our knowledge, direct physical interaction with purified tubulin has previously been shown only for M proteins of Sendai virus (42) and the Indiana serotype of vesicular stomatitis virus (34). Our data indicate a direct association between Ebola VP40 and tubulin (Fig. 3) both in vivo and in vitro. Furthermore, purified full-length VP40, when added to tubulin in vitro, enhanced polymerization of tubulin, suggesting that the MT bundling seen in vivo probably is not dependent on an intermediary protein. This is the first report of an animal viral protein directly augmenting tubulin polymerization in vitro. However, a recent report indicates in vitro induction of tubulin polymerization by potato X virus (51).

Our findings suggest that VP40 exhibits the properties of a microtubule-associated protein (MAP), that is, it binds to tubulin and affects its polymerization and dynamics. The mechanism of this physical association is presently not clear. Our findings indicate that eliminating the C-terminal 18 amino acids of VP40 completely eliminated the association of VP40 with microtubules. However, when the C-terminal tail of VP40 was fused to red fluorescence protein and expressed in cells, it failed to exhibit a fibrillar expression pattern (data not shown). Studies with purified protein (50) previously demonstrated that removing the C-terminal tail of VP40 destabilizes the two domains of the protein and significantly alters the conformation. Consistent with these reports, our studies in transfected cells showed that truncating the C-terminal 18 amino acids of VP40 resulted in premature oligomerization, cytoplasmic retention, and elimination of virus-like particle release (43). The likelihood that the loss of microtubule association in $VP40_{1–308}$ was a result of a conformation change suggests that the association of VP40 with tubulin could be governed by a conformational surface consisting of multiple motifs.

The pattern of microtubule bundling induced by VP40 is reminiscent of microtubule stabilization triggered by the microtubule-associated proteins MAP2 and Tau, a phenomenon thought to support neuronal process outgrowth (15, 23). Mutational analyses have demonstrated that microtubule binding and bundling activities of MAP2 was dependent on a 31-amino-acid motif imperfectly repeated in tandem in the carboxy terminus of MAP2 (15), with the strength of binding being dependent on the number of these repeats. Our sequence alignment of Ebola VP40 with MAP2 revealed a region in the C-terminal domain of VP40 (amino acids 223 to 253) that exhibited 35% sequence identity with the fourth 31-amino-acid repeat of MAP2 (Fig. 7A). This motif is also present in the microtubule-associated protein Tau (39 to 62% sequence identity with the different MAP2 repeats). When we deleted sequences corresponding to this motif in VP40, it resulted in loss of microtubule association and bundling (Fig. 7C), suggesting that a mechanism similar to MAP2 may be involved in VP40 interactions with tubulin. This motif forms a large exposed surface on the VP40 molecule (Fig. 7B), suggesting its accessibility for interactions with tubulin. We also found small patches of sequence identity between the first and second repeat and regions in the N-terminal domain of VP40, the significance of which remains to be investigated (data not shown). Interestingly, the 31-amino-acid motif is not present in Marburg virus VP40, and in preliminary experiments, we were unable to detect any microtubule bundling in Marburg virus VP40-transfected cells (data not shown). It remains to be determined whether this reflects a mechanistic difference between the life cycle of these two related viruses.

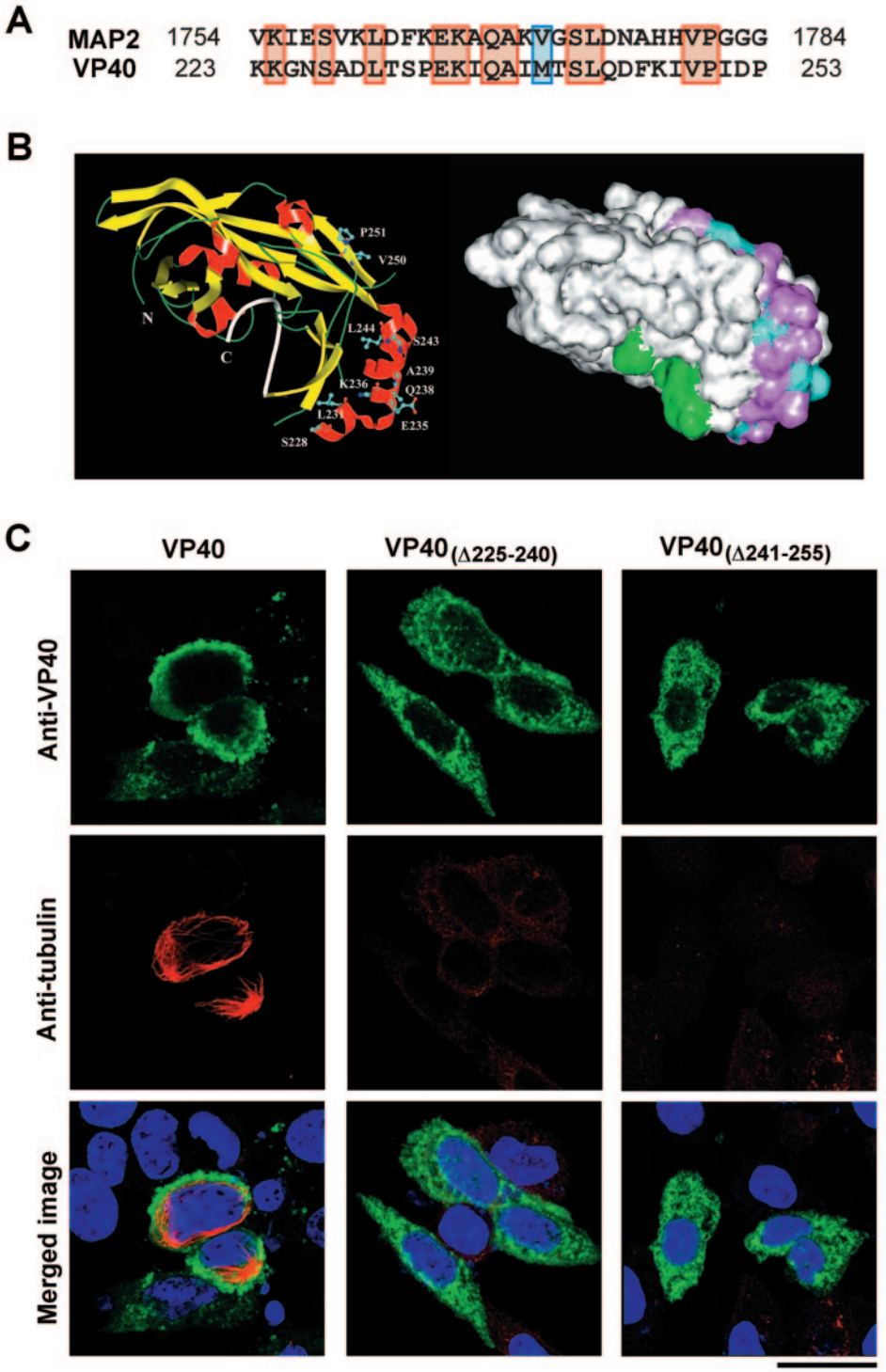

FIG. 7. Sequence similarity to a microtubule-associated protein motif suggests a structural basis for VP40 association with tubulin. (A) Alignment of VP40 amino acids 223 to 253 with the fourth tubulin binding repeat of MAP2. The orange background indicates identical residues, and blue indicates homologous residues. (B) The MAP2 tubulin binding motif in the X-ray structure of VP40 (amino acids 44 to 321). (Left) Ribbon diagram of VP40 with helical, sheet, and loop structures colored red, yellow, and green, respectively, except for the C-terminal loop residues 308 to 321, which are colored white. Residues 223 to 254 form α-helices 5 and 6 and β-strand 9. To highlight the common residues between MAP2 and VP40, amino acids S228, L231, E235, Q238, A239, S243, L244, V250, and P251 are additionally rendered in ball-and-stick format (cyan, carbon atoms; red, oxygen atoms; blue, nitrogen atoms). K225 is not shown because it is untraceable in the X-ray structure. (Right) In the same orientation as the ribbon diagram, VP40 is shown as a surface rendering. Residues 223 to 254 are colored purple, with the common MAP2/VP40 residues colored cyan. The amino acid segment 223 to 254 is largely solvent exposed and thus provides a binding surface for tubulin. The C-terminal residues 308 to 321 are colored green. (C) Full-length VP40 and two VP40 mutants with deletions in the motif region were transfected into 293T cells, which were treated with 10 μM nocodazole for 2 h before fixation. Cells were stained with antibodies to VP40 (green) and α-tubulin (red) and labeled with Hoechst dye (blue). Unlike full-length VP40, neither of the deletion mutants protected microtubules from depolymerization. Bar, 20 μm.

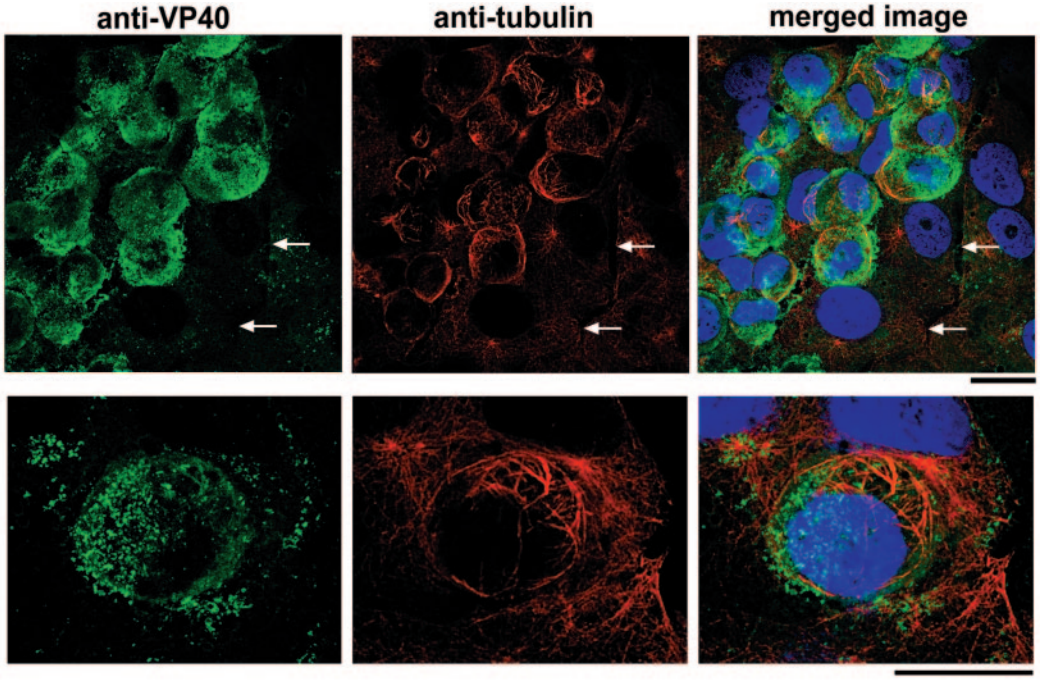

FIG. 8. Effect of Ebola virus infection on microtubule arrangement and stability. Vero-E6 cells were infected with Ebola virus and treated with nocodazole (2 μM) after 48 h. After fixation and irradiation, cells were immunostained for VP40 (green) and α-tubulin (red). Cells were also treated with Hoechst stain (blue) to label cell nuclei. Infected cells that stained heavily for VP40 (upper left of top panels) contained numerous microtubule bundles compared to neighboring cell populations that did not exhibit high levels of VP40 staining (two cells that did not stain for VP40 are marked by arrows). For better visualization of the microtubule bundling, a higher-magnification view of Ebola-infected cells is shown in the bottom panels. Bars, 20 μm.

Ferralli and colleagues reported that the tubulin binding repeats alone are not sufficient for microtubule bundling and that flanking sequences, which include proline-rich regions N-terminal to the repeats, are critical for binding and bundling (15). Proline-rich sequences have also been recognized in other MAPs (23, 27, 56). VP40 also contains several proline-rich sequences in the N-terminal domain, suggesting that the microtubule binding may result from coordinated action of the 31-amino-acid motif and the proline-rich sequences. The conformational change resulting from the deletion of the C-terminal tail of VP40 may severely alter the coordination of these motifs with respect to each other, leading to loss of the microtubule binding surface. Furthermore, ionic interactions between the basic patches of Ebola VP40 (11) and acidic regions of tubulin may contribute to these interactions as suggested for vesicular stomatitis virus and Sendai virus M proteins (34, 42). Therefore the interaction between tubulin and VP40 may be complex and its precise mechanism remains to be determined by more detailed and targeted mutational analyses.

Although the ability of purified VP40 to bind to purified tubulin (Fig. 3) and to enhance the polymerization of tubulin in an in vitro assay (Fig. 6) indicates a direct interaction between the two proteins, this does not preclude the possibility of an additional affinity for a motor protein. Involvement of a motor protein would be expected for directed transport along microtubules. Microtubules are polarized structures, and the direction of movement along them is a function of the associated motor proteins. Binding to the minus-end-directed motor protein dynein has been reported for African swine fever virus protein 54 (1) as well as VP26 of herpes simplex virus (12), and binding to members of the plus-end directed kinesin family of motor proteins has been demonstrated for the vaccinia virus protein A36R (47, 57) and murine leukemia virus Gag proteins (24). Bidirectional movement along microtubules, believed to be the result of two competing motor activities, has been described for adenovirus (53). Inwardly directed movement along microtubules is unlikely to be of great importance for EBOV because, as a negative-strand RNA virus, it does not need to make its way into the nucleus for replication. However, viral progeny must reach the plasma membrane to bud from the cell surface. Therefore, a microtubule association may conceivably be equally important for the egress of viruses that replicate in the cytoplasm. Use of microtubules and associated motor proteins for movement of viral particles to the site of budding has been proposed for African swine fever virus and vaccinia virus (22, 36). It is intriguing that the VP40 deletion mutants that did not cause microtubule bundling also failed to associate with the plasma membrane (Fig. 7C). While this finding suggests a possible role for microtubules in VP40 membrane translocation, more detailed studies and conclusive evidence are needed to ascertain a direct relationship.

Our present and previous studies demonstrated that VP40 is found both in the cytoplasm (43) and plasma membrane, a property shared with matrix proteins of Marburg virus (25), Sendai virus (26), and parainfluenza virus (8). The cytoplasmic pool of VP40 bound to microtubules may provide a link between the ribonucleocapsid assembly and the envelope assembly believed to be driven by membrane-associated VP40 (2).

Microtubules have been reported to be involved in viral transcription of negative-strand RNA viruses such as Sendai virus, vesicular stomatitis virus, and measles virus (37, 38). M proteins of vesicular stomatitis virus, Sendai virus, rabies, measles, and influenza virus are known to cease transcription, allowing the assembly process to be initiated (6, 9, 20, 35, 42, 54, 58). Microtubule binding of Sendai virus M protein has been shown to remove the inhibitory effect of M protein on viral transcription (42). It remains to be seen whether filoviral matrix proteins also use this common mechanism of *Mononegavirales*. Studies are under way in our laboratory to examine this possibility.

In summary, our data suggest that EBOV uses cellular microtubules during its life cycle. These findings add this filovirus to a growing list of viruses that have evolved mechanisms to exploit cytoskeletal components to their own advantage. Future studies should reveal the detailed mechanism of this interaction and its functional consequence for the biology of EBOV. Understanding the cellular components that the virus relies on for replication is essential for devising strategies for therapeutic intervention. In this regard, microtubules may be an important therapeutic target. In particular, conservation of this pathway among multiple viruses suggests that therapeutic strategies aimed at such cellular machineries may lead to development of broad-spectrum antivirals.

ACKNOWLEDGMENTS

We thank Roger Tsien, Guido M. Gaietta, and Mark Ellisman (National Center for Microscopy and Imaging Research, La Jolla, Calif., which is supported by NIH Center for Research Resources Grant P41-04050 to M. Ellisman) for valuable advice regarding imaging with biarsenic dyes. We also thank Diane Negely and Dan Lackner (USAMRIID) for assistance with virus infection.

This work was supported by the US Army Medical Research and Materiel Command Research Plan 03-4-4J-012.

REFERENCES

1. **Alonso, C., J. Miskin, B. Hernaez, P. Fernandez-Zapatero, L. Soto, C. Canto, I. Rodriguez-Crespo, L. Dixon, and J. M. Escribano.** 2001. African swine fever virus protein p54 interacts with the microtubular motor complex through direct binding to light-chain dynein. J. Virol. **75:**9819–9827.
2. **Aman, M. J., C. M. Bosio, R. G. Panchal, J. C. Burnett, A. Schmaljohn, and S. Bavari.** 2003. Molecular mechanisms of filovirus cellular trafficking. Microbes Infect. **5:**639–649.
3. **Bailey, C. J., R. G. Crystal, and P. L. Leopold.** 2003. Association of adenovirus with the microtubule organizing center. J. Virol. **77:**13275–13287.
4. **Bavari, S., C. M. Bosio, E. Wiegand, G. Ruthel, A. B. Will, T. W. Geisbert, M. Hevey, C. Schmaljohn, A. Schmaljohn, and M. J. Aman.** 2002. Lipid raft microdomains: a gateway for compartmentalized trafficking of Ebola and Marburg viruses. J. Exp. Med. **195:**593–602.
5. **Broering, T. J., J. S. Parker, P. L. Joyce, J. Kim, and M. L. Nibert.** 2002. Mammalian reovirus nonstructural protein microNS forms large inclusions and colocalizes with reovirus microtubule-associated protein micro2 in transfected cells. J. Virol. **76:**8285–8297.
6. **Carroll, A. R., and R. R. Wagner.** 1979. Role of the membrane (M) protein in endogenous inhibition of in vitro transcription by vesicular stomatitis virus. J. Virol. **29:**134–142.
7. **Chiou, C. T., C. C. Hu, P. H. Chen, C. L. Liao, Y. L. Lin, and J. J. Wang.** 2003. Association of Japanese encephalitis virus NS3 protein with microtubules and tumour susceptibility gene 101 (TSG101) protein. J. Gen. Virol. **84:**2795–2805.
8. **Coronel, E. C., T. Takimoto, K. G. Murti, N. Varich, and A. Portner.** 2001. Nucleocapsid incorporation into parainfluenza virus is regulated by specific interaction with matrix protein. J. Virol. **75:**1117–1123.
9. **De, B. P., G. B. Thornton, D. Luk, and A. K. Banerjee.** 1982. Purified matrix protein of vesicular stomatitis virus blocks viral transcription in vitro. Proc. Natl. Acad. Sci. USA **79:**7137–7141.
10. **de Matos, A. P., and Z. G. Carvalho.** 1993. African swine fever virus interaction with microtubules. Biol. Cell **78:**229–234.
11. **Dessen, A., E. Forest, V. Volchkov, O. Dolnik, H. D. Klenk, and W. Weissenhorn.** 2000. Crystallization and preliminary X-ray analysis of the matrix protein from Ebola virus. Acta Crystallogr. D **56:**758–760.
12. **Douglas, M. W., R. J. Diefenbach, F. L. Homa, M. Miranda-Saksena, F. J. Rixon, V. Vittone, K. Byth, and A. L. Cunningham.** 2004. Herpes simplex virus type 1 capsid protein VP26 interacts with dynein light chains RP3 and Tctex1 and plays a role in retrograde cellular transport. J. Biol. Chem. **279:**28522–28530.
13. **Elliott, G., and P. O'Hare.** 1998. Herpes simplex virus type 1 tegument protein VP22 induces the stabilization and hyperacetylation of microtubules. J. Virol. **72:**6448–6455.
14. **Feldmann, H., and M. P. Kiley.** 1999. Classification, structure, and replication of filoviruses. Curr. Top. Microbiol. Immunol. **235:**1–21.
15. **Ferralli, J., T. Doll, and A. Matus.** 1994. Sequence analysis of MAP2 function in living cells. J. Cell Sci. **107:**3115–3125.
16. **Gaietta, G., T. J. Deerinck, S. R. Adams, J. Bouwer, O. Tour, D. W. Laird, G. E. Sosinsky, R. Y. Tsien, and M. H. Ellisman.** 2002. Multicolor and electron microscopic imaging of connexin trafficking. Science **296:**503–507.
17. **Garoff, H., R. Hewson, and D. J. Opstelten.** 1998. Virus maturation by budding. Microbiol. Mol. Biol. Rev. **62:**1171–1190.
18. **Gomis-Ruth, F. X., A. Dessen, J. Timmins, A. Bracher, L. Kolesnikowa, S. Becker, H. D. Klenk, and W. Weissenhorn.** 2003. The matrix protein VP40 from Ebola virus octamerizes into pore-like structures with specific RNA binding properties. Structure (Cambridge) **11:**423–433.
19. **Harty, R. N., M. E. Brown, G. Wang, J. Huibregtse, and F. P. Hayes.** 2000. A PPxY motif within the VP40 protein of Ebola virus interacts physically and functionally with a ubiquitin ligase: implications for filovirus budding. Proc. Natl. Acad. Sci. USA **97:**13871–13876.
20. **Ito, Y., A. Nishizono, K. Mannen, K. Hiramatsu, and K. Mifune.** 1996. Rabies virus M protein expressed in Escherichia coli and its regulatory role in virion-associated transcriptase activity. Arch. Virol. **141:**671–683.
21. **Jasenosky, L. D., G. Neumann, I. Lukashevich, and Y. Kawaoka.** 2001. Ebola virus VP40-induced particle formation and association with the lipid bilayer. J. Virol. **75:**5205–5214.
22. **Jouvenet, N., P. Monaghan, M. Way, and T. Wileman.** 2004. Transport of African swine fever virus from assembly sites to the plasma membrane is dependent on microtubules and conventional kinesin. J. Virol. **78:**7990–8001.
23. **Kanai, Y., J. Chen, and N. Hirokawa.** 1992. Microtubule bundling by tau proteins in vivo: analysis of functional domains. EMBO J. **11:**3953–3961.
24. **Kim, W., Y. Tang, Y. Okada, T. A. Torrey, S. K. Chattopadhyay, M. Pfleiderer, F. G. Falkner, F. Dorner, W. Choi, N. Hirokawa, and H. C. Morse III.** 1998. Binding of murine leukemia virus Gag polyproteins to KIF4, a microtubule-based motor protein. J. Virol. **72:**6898–6901.
25. **Kolesnikova, L., H. Bugany, H. D. Klenk, and S. Becker.** 2002. VP40, the matrix protein of Marburg virus, is associated with membranes of the late endosomal compartment. J. Virol. **76:**1825–1838.
26. **Lamb, R. A., and P. W. Choppin.** 1977. The synthesis of Sendai virus polypeptides in infected cells. II. Intracellular distribution of polypeptides. Virology **81:**371–381.
27. **Lewis, S. A., D. H. Wang, and N. J. Cowan.** 1988. Microtubule-associated protein MAP2 shares a microtubule binding motif with tau protein. Science **242:**936–939.
28. **Licata, J. M., M. Simpson-Holley, N. T. Wright, Z. Han, J. Paragas, and R. N. Harty.** 2003. Overlapping motifs (PTAP and PPEY) within the Ebola virus VP40 protein function independently as late budding domains: involvement of host proteins TSG101 and VPS-4. J. Virol. **77:**1812–1819.
29. **Ludin, B., K. Ashbridge, U. Funfschilling, and A. Matus.** 1996. Functional analysis of the MAP2 repeat domain. J. Cell Sci. **109:**91–99.
30. **Luftig, R. B.** 1982. Does the cytoskeleton play a significant role in animal virus replication? J. Theor. Biol. **99:**173–191.
31. **Luftig, R. B., and R. R. Weihing.** 1975. Adenovirus binds to rat brain microtubules in vitro. J. Virol. **16:**696–706.
32. **Martin, A., P. O'Hare, J. McLauchlan, and G. Elliott.** 2002. Herpes simplex virus tegument protein VP22 contains overlapping domains for cytoplasmic localization, microtubule interaction, and chromatin binding. J. Virol. **76:**4961–4970.
33. **Martin-Serrano, J., T. Zang, and P. D. Bieniasz.** 2001. HIV-1 and Ebola virus encode small peptide motifs that recruit Tsg101 to sites of particle assembly to facilitate egress. Nat. Med. **7:**1313–1319.
34. **Melki, R., Y. Gaudin, and D. Blondel.** 1994. Interaction between tubulin and the viral matrix protein of vesicular stomatitis virus: possible implications in the viral cytopathic effect. Virology **202:**339–347.
35. **Mizumoto, K., K. Muroya, T. Takagi, T. Omata-Yamada, H. Shibuta, and K. Iwasaki.** 1995. Protein factors required for in vitro transcription of Sendai virus genome. J. Biochem. (Tokyo) **117:**527–534.
36. **Moss, B., and B. M. Ward.** 2001. High-speed mass transit for poxviruses on microtubules. Nat. Cell Biol. **3:**E245–E246.
37. **Moyer, S. A., S. C. Baker, and S. M. Horikami.** 1990. Host cell proteins required for measles virus reproduction. J. Gen. Virol. **71:**775–783.
38. **Moyer, S. A., S. C. Baker, and J. L. Lessard.** 1986. Tubulin: a factor necessary for the synthesis of both Sendai virus and vesicular stomatitis virus RNAs. Proc. Natl. Acad. Sci. USA **83:**5405–5409.
39. **Nejmeddine, M., G. Trugnan, C. Sapin, E. Kohli, L. Svensson, S. Lopez, and**

J. Cohen. 2000. Rotavirus spike protein VP4 is present at the plasma membrane and is associated with microtubules in infected cells. J. Virol. **74:** 3313–3320.
40. **Obuchi, M., T. Odagiri, K. Asakura, and Y. Ohara.** 2001. Association of L* protein of Theiler's murine encephalomyelitis virus with microtubules in infected cells. Virology **289:**95–102.
41. **O'Donnell, L. A., J. A. Clemmer, K. Czymmek, and C. J. Schmidt.** 2002. Marek's disease virus VP22: subcellular localization and characterization of carboxyl terminal deletion mutations. Virology **292:**235–240.
42. **Ogino, T., M. Iwama, Y. Ohsawa, and K. Mizumoto.** 2003. Interaction of cellular tubulin with Sendai virus M protein regulates transcription of viral genome. Biochem. Biophys. Res. Commun. **311:**283–293.
43. **Panchal, R. G., G. Ruthel, T. A. Kenny, G. H. Kallstrom, D. Lane, S. S. Badie, L. Li, S. Bavari, and M. J. Aman.** 2003. In vivo oligomerization and raft localization of Ebola virus protein VP40 during vesicular budding. Proc. Natl. Acad. Sci. USA **100:**15936–15941.
44. **Parker, J. S., T. J. Broering, J. Kim, D. E. Higgins, and M. L. Nibert.** 2002. Reovirus core protein mu2 determines the filamentous morphology of viral inclusion bodies by interacting with and stabilizing microtubules. J. Virol. **76:** 4483–4496.
45. **Petit, C., M. L. Giron, J. Tobaly-Tapiero, P. Bittoun, E. Real, Y. Jacob, N. Tordo, H. De The, and A. Saib.** 2003. Targeting of incoming retroviral Gag to the centrosome involves a direct interaction with the dynein light chain 8. J. Cell Sci. **116:**3433–3442.
46. **Ploubidou, A., and M. Way.** 2001. Viral transport and the cytoskeleton. Curr. Opin. Cell Biol. **13:**97–105.
47. **Rietdorf, J., A. Ploubidou, I. Reckmann, A. Holmstrom, F. Frischknecht, M. Zettl, T. Zimmermann, and M. Way.** 2001. Kinesin-dependent movement on microtubules precedes actin-based motility of vaccinia virus. Nat. Cell Biol. **3:**992–1000.
48. **Ruigrok, R. W., G. Schoehn, A. Dessen, E. Forest, V. Volchkov, O. Dolnik, H. D. Klenk, and W. Weissenhorn.** 2000. Structural characterization and membrane binding properties of the matrix protein VP40 of Ebola virus. J. Mol. Biol. **300:**103–112.
49. **Sanderson, C. M., M. Hollinshead, and G. L. Smith.** 2000. The vaccinia virus A27L protein is needed for the microtubule-dependent transport of intracellular mature virus particles. J. Gen. Virol. **81:**47–58.
50. **Scianimanico, S., G. Schoehn, J. Timmins, R. H. Ruigrok, H. D. Klenk, and W. Weissenhorn.** 2000. Membrane association induces a conformational change in the Ebola virus matrix protein. EMBO J. **19:**6732–6741.
51. **Serazev, T. V., N. O. Kalinina, E. S. Nadezhdina, N. A. Shanina, and S. Y. Morozov.** 2003. Potato virus X coat protein interacts with microtubules in vitro. Cell Biol. Int. **27:**271–272.
52. **Sodeik, B.** 2000. Mechanisms of viral transport in the cytoplasm. Trends Microbiol. **8:**465–472.
53. **Suomalainen, M., M. Y. Nakano, S. Keller, K. Boucke, R. P. Stidwill, and U. F. Greber.** 1999. Microtubule-dependent plus- and minus end-directed motilities are competing processes for nuclear targeting of adenovirus. J. Cell Biol. **144:**657–672.
54. **Suryanarayana, K., K. Baczko, V. ter Meulen, and R. R. Wagner.** 1994. Transcription inhibition and other properties of matrix proteins expressed by M genes cloned from measles viruses and diseased human brain tissue. J. Virol. **68:**1532–1543.
55. **Timmins, J., S. Scianimanico, G. Schoehn, and W. Weissenhorn.** 2001. Vesicular release of Ebola virus matrix protein VP40. Virology **283:**1–6.
56. **Wallin, M., J. Deinum, L. Goobar, and U. H. Danielson.** 1990. Proteolytic cleavage of microtubule-associated proteins by retroviral proteinases. J. Gen. Virol. **71:**1985–1991.
57. **Ward, B. M., and B. Moss.** 2004. Vaccinia virus A36R membrane protein provides a direct link between intracellular enveloped virions and the microtubule motor kinesin. J. Virol. **78:**2486–2493.
58. **Watanabe, K., H. Handa, K. Mizumoto, and K. Nagata.** 1996. Mechanism for inhibition of influenza virus RNA polymerase activity by matrix protein. J. Virol. **70:**241–247.